Electronic Supplementary Material (ESI) for Chemical Communications

Novel polyoxometalate–phosphazene aggregates and their use as catalysts for biphasic oxidations with hydrogen peroxide

Michael Craven, Rana Yahya, Elena Kozhevnikova, Ramamoorthy Boomishankar, Craig M. Robertson, Alexander Steiner, and Ivan Kozhevnikov

Electronic Supporting Information

Experimental Section

Crystallographic data

Thermal Gravimetric Analysis of POM–RPN aggregates

UV/Vis and FTIR spectra of POM–RPN aggregates

Kinetics of DBT oxidation

Catalyst recovery and reuse

Experimental Section

Phosphazenes **RPN** were synthesised as reported previously.[S1] POM–phosphazene aggregates were obtained by dissolving heteropoly acid hydrates (0.1 mmol) and phosphazenes (0.3 – 0.6 mmol) in methanol at 40°C. The salt aggregates were crystallised upon slow evaporation of the solvent at room temperature and isolated by filtration using a Büchner funnel. CHN elemental analysis was in agreement with the compositions of POM-phosphazene aggregates.

Elemental analysis

[**iBuPN**H]$_4$[**SiW**]·2CH_3OH. Found C, 22.25; H, 4.80; N, 9.60. Calcd for $C_{98}H_{252}N_{36}O_{42}P_{12}SiW_{12}$: C, 22.58; H, 4.87; N, 9.67.

[**iBuPN**H][**iBuPN**H_2][**PW**]·CH_3OH·3H_2O. Found C, 14.31; H, 2.98; N, 6.14. Calcd for $C_{98}H_{252}N_{36}O_{42}P_{12}SiW_{12}$: C, 14.35; H, 3.27; N, 6.15.

The oxidation of DBT and epoxidation of cyclooctene were carried out in two-phase system containing toluene as an organic solvent and aqueous H_2O_2 at 25-60°C in a 50-mL glass reactor equipped with a magnetic stirrer and a reflux condenser. In a typical run, toluene (10 mL), the substrate (DBT or cyclooctene), dodecane (GC internal standard), **RPN** and aqueous H_2O_2 in specified quantities were added into reactor. Once the reactor was heated to the required temperature, heteropoly acid was added to start the reaction. Blank experiments showed that no reaction occurred in the absence of POM. The reactions were monitored by taking aliquots from the organic phase and submitting them to GC analysis (Varian CP-3380 gas chromatograph equipped with FID and a 25 m × 0.32 mm × 0.5 μm BP1 capillary column) to determine substrate conversion and product yield. After reaction, the amount of remaining H_2O_2 was determined by titration with $KMnO_4$. This allowed the efficiency of hydrogen peroxide use to be estimated.

S1 A. Steiner, in *Polyphosphazenes for Biomedical Applications* (Ed: A. K. Adrianov), WILEY, New Jersey, 2009, pp. 411-453.

Crystallographic data

Reflections were collected on a Bruker Smart Apex diffractometer using MoK_α radiation (λ = 0.71073 Å). Structures were refined by full-matrix least-squares against F^2 using all data.[S2] Absorption corrections were carried out using redundant reflections obtained from multi-scans. W, Si and P atoms were refined aniostropically, all other atoms were refined isotropically. H-atoms were fixed in calculated positions. The central atoms of the polyanions (Si and P, respectively) reside on crystallographic inversion centres. As a result, the O-atoms of the central SiO_4 and PO_4 tetrahedra are disordered over two positions and were refined with half occupancies. Crystals of [**iBuPN**H]$_4$[**SiW**]·2CH_3OH diffracted weakly lacking detectable reflections at higher 2θ angles, thus the data were truncated at 1.00 Å and the atom positions of the alkyl groups were refined with similar-distance and similar-U restraints. CCDC 892678 - 892680, contain the supplementary crystallographic data. These can be obtained free of charge *via* www.ccdc.cam.ac.uk/conts/retrieving.html (or from The Cambridge Crystallographic Data Centre, 12 Union Road, Cambridge CB2 1EZ, UK; fax: +44 1223 336 033; deposit@ccdc.cam.ac.uk).

[**iBuPN**H]$_4$[**SiW**]·2CH_3OH: $C_{98}H_{252}N_{36}O_{42}P_{12}SiW_{12}$, M_r = 5213.25, T = 100 K, $P2_1/n$, a = 20.110(3), b = 18.245(3), c = 24.298(4) Å, β = 108.202(2)°, V = 8469(2) Å^3, Z = 2, ρ = 2.044 g cm^{-3}, reflections, total = 36130, unique = 8788, $2\theta_{max}$ = 41.64°, $R1$ ($I > 2\sigma(I)$) = 0.066, $wR2$ (all data) = 0.191.

[**iPrPN**H][**iPrPN**H_2][**PW**]·6CH_3OH: $C_{42}H_{123}N_{18}O_{46}P_7W_{12}$, M_r = 4039.57, T = 100 K, $P2_1/n$, a = 14.6216(12), b = 23.3093(19), c = 15.2198(12) Å, β = 107.725(2)°, V = 4941.0(7) Å^3, Z = 2, ρ = 2.715 g cm^{-3}, reflections, total = 57225, unique = 8706, $2\theta_{max}$ = 50.04°, $R1$ ($I > 2\sigma(I)$) = 0.089, $wR2$ (all data) = 0.198.

[**iBuPN**H][**iBuPN**H_2][**PW**]·CH_3OH·3H_2O: $C_{49}H_{133}N_{18}O_{44}P_7W_{12}$, M_r = 4101.72, T = 100 K, P-1, a = 11.9608(15), b = 12.2067(15), c = 19.129(2) Å, α = 83.566(2), β = 82.709(2), γ = 71.195(2)°, V = 2614.8(6) Å^3, Z = 1, ρ = 2.605 g cm^{-3}, reflections, total = 22675, unique = 9188, $2\theta_{max}$ = 50.06°, $R1$ ($I > 2\sigma(I)$) = 0.082, $wR2$ (all data) = 0.185.

S2 G.M. Sheldrick, *Acta Crystallogr.* 2008, **A64**, 112.

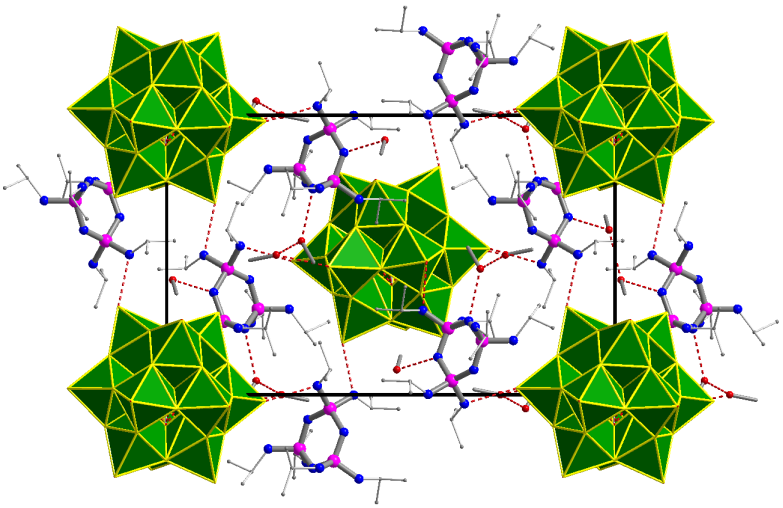

Figure S1 Crystal packing diagram of [**iPrPN**H][**iPrPN**H_2][**PW**]·6CH_3OH.

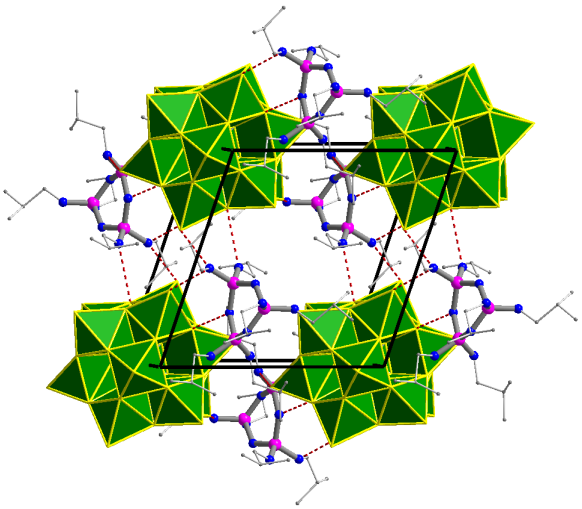

Figure S2 Crystal packing diagram of [**iBuPN**H][**iBuPN**H_2][**PW**]·CH_3OH·3H_2O.

[**iBuPN**H]$_3$[**PW**]·3**iBuPN**H·*x* solvent: Several crystallization trials were carried out on batches containing H_3**PW** and **RPN** in a 1:6 ratio, all of which produced crystals exhibiting a high degree of mosaicity. Batches with **iBuPN** gave crystals of sufficient quality to allow indexing of reflections giving a monoclinic *C*-centred cell: a = 32.94(3), b = 29.64(2), c = 21.46(2) Å, β = 96.102(10)°, V = 2083(3) Å^3; the systematic absences indicated a *c*-glide plane. A reasonable structure solution was obtained in spacegroup *C*2/*c*. However, due to the poor quality of the crystal only the positions of W and P atoms could be determined. The six unique W positions were obtained from the Patterson map. These are part of the W_{12} frame of the polyoxometalate cluster, which is located on a crystallographic inversion centre. Subsequent Fourier difference maps revealed the positions of the P atoms of the three unique phosphazene ligands clearly visible as triangular P_3 arrangements. After the next round of refinements N-atoms appeared in the difference map. However, the N-atoms were only stable in subsequent refinement cycles with the use of heavy restraints. The model shown in Fig. 2b was generated by fitting idealized P_3N_9 (D_{3h}) and $PW_{12}O_{40}$ (O_h) fragments onto the P_3 and W_{12} clusters. While the X-ray structure confirms the 1:6 ratio of POM to phosphazene ligands and also gives a rough indication of their spatial arrangement in the cell, the poor quality of the data prohibits a more detailed structural analysis. Considering the presence of [**PW**]$^{3-}$ ions, the most likely composition of these crystals is [**iBuPN**H]$_3$[**PW**]·3**iBuPN**·*x* solvent containing both cationic and neutral phosphazene ligands. This arrangement is not compatible with the inversion symmetry and must therefore involve disorder where cationic and neutral ligands partially occupy the same sites (the refinement in the acentric spacegroup *Cc* is unstable). One can assume that **RPN** and **RPN**H$^+$ have similar though not identical H-bonding requirements. This allows them to occupy crystallographically equivalent sites, albeit with slightly different atom positions to faciliate optimum intermolecular interactions. The mosaic character of the crystals might well be a result of this disorder. CCDC 907986 contains the supplementary crystallographic data.

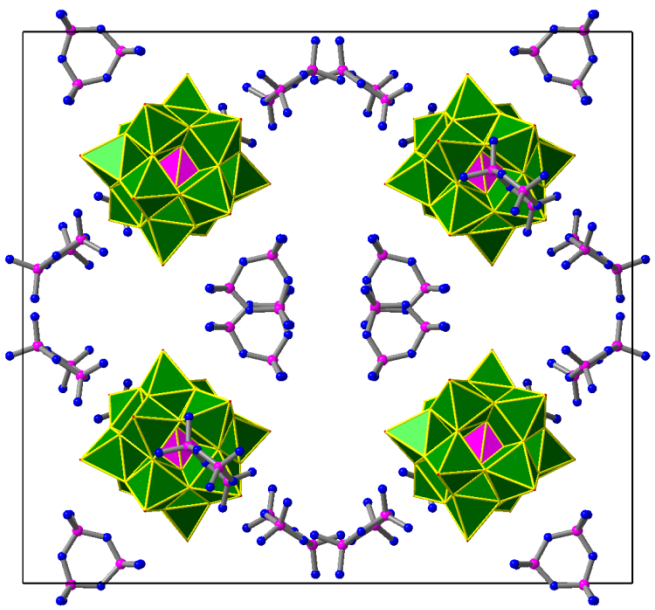

Figure S3 Crystal packing diagram of [**iBuPN**H]$_3$[**PW**]·3**iBuPN**H·*x* solvent.

Thermal Gravimetric Analysis of POM–RPN aggregates

The TGA for **iPrPN** and **iBuPN** as well as for the corresponding POM aggregates was performed under nitrogen on a Perkin-Elmer TGA 7 instrument. The results are shown in Figures S4-S6. It can be seen that these phosphazenes decompose at ~300°C, with a decomposition onset at 150°C for **iPrPN** and 180°C for **iBuPN**. The corresponding POM–**RPN** composites exhibited higher thermal stability, showing decomposition onsets at 260°C for **PW–iPrPN** and 280°C for **PW–iBuPN**. The **SiW–iBuPN** composite had even higher thermal stability, with a decomposition onset at 340°C (Figure S6).

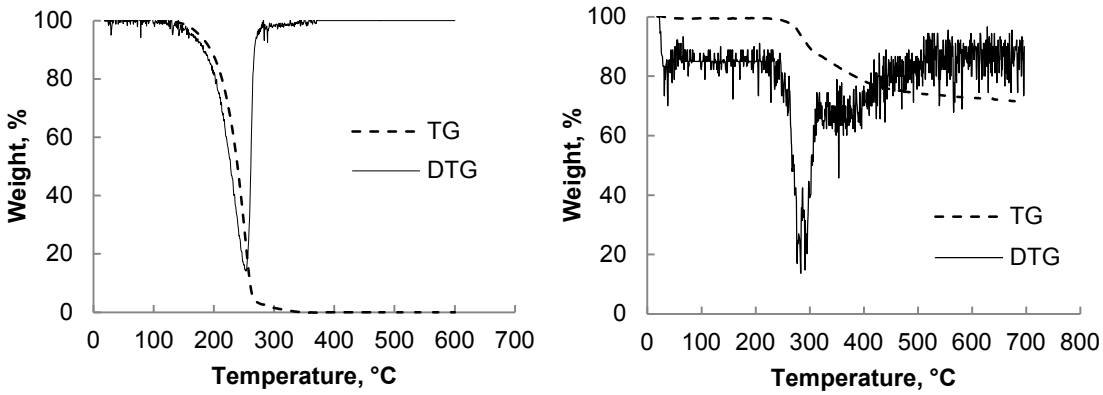

Figure S4 TGA for **iPrPN** (left) and **PW-iPrPN** (right) under N_2.

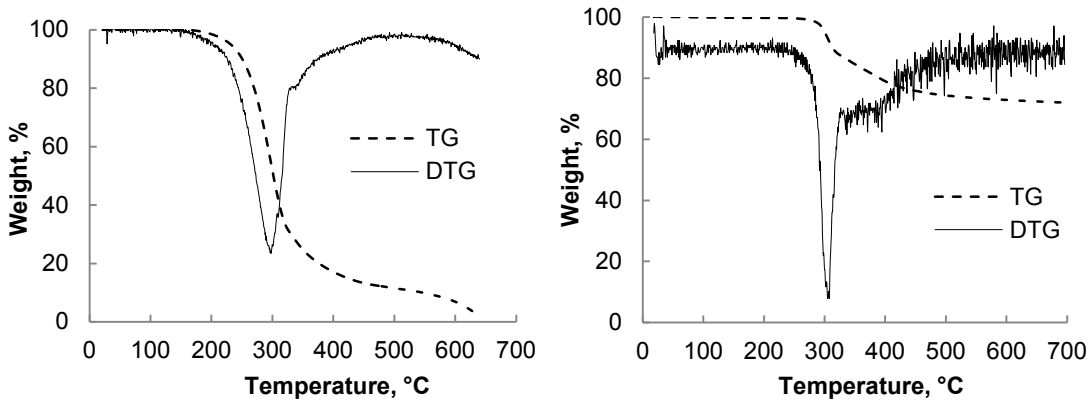

Figure S5 TGA for **iBuPN** (left) and **PW–iBuPN** (right) under N_2.

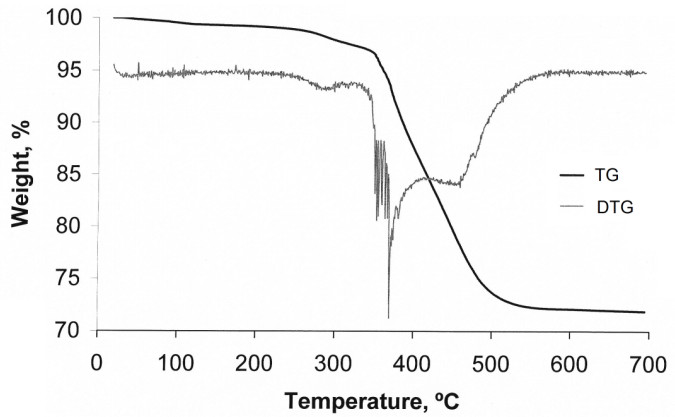

Figure S6 TGA for **SiW–iBuPN** under N_2.

UV/Vis and FTIR spectra of POM–RPN aggregates

Figure S7 shows the UV/Vis spectrum of **SiW–iBuPN** aggregate in comparison with the spectrum of **SiW** in MeOH solution. Both spectra exhibit the same strong charge-transfer band of the **SiW** polyanion at 265 nm. This implies that the electron structure of **SiW** is practically unaffected by interaction with **iBuPN**. Similarly, **PW** and **SiW** aggregates exhibited practically unchanged FTIR bands characteristic of the Keggin POMs (Figure S8), thus confirming that the state of POM is little affected by the presence of hydrogen bonded phosphazene cations.

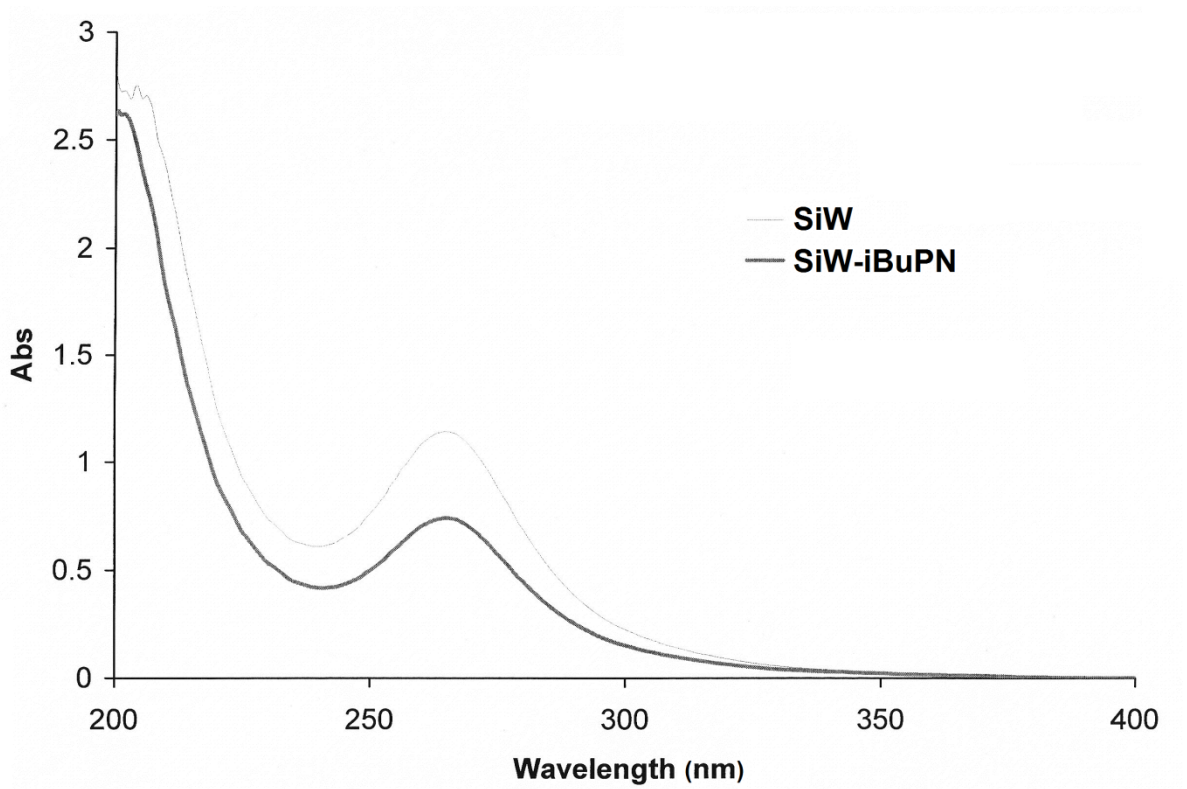

Figure S7 UV-Vis spectra of **SiW** (0.028 mM, $\varepsilon_{265} = 5.05 \cdot 10^4$ $M^{-1}cm^{-1}$) and **SiW–iBuPN** (0.019 mM, $\varepsilon_{265} = 5.05 \cdot 10^4$ $M^{-1}cm^{-1}$) in MeOH showing the **SiW** absorption band at 265 nm.

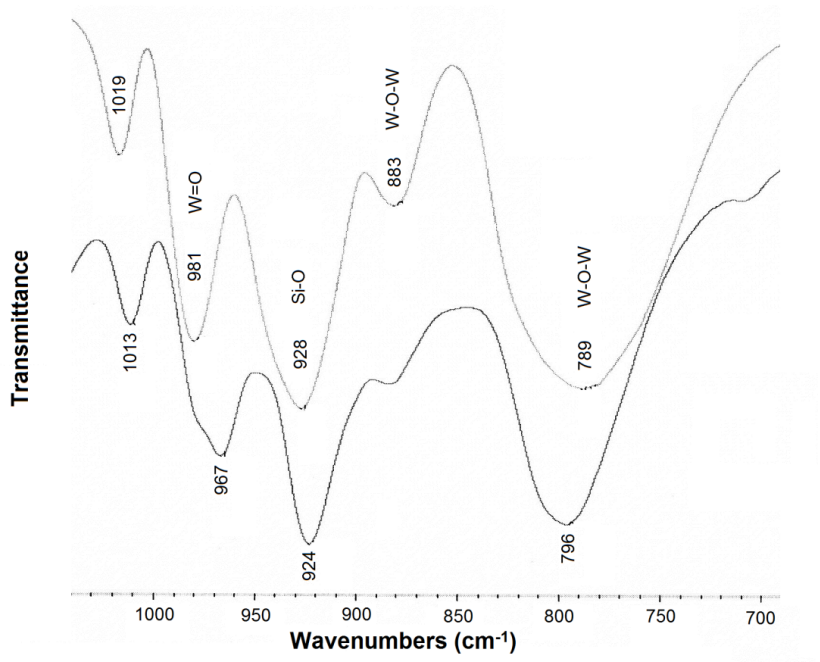

Figure S8 FTIR spectra of **SiW** (top) and **SiW–iBuPN** (bottom).

Kinetics of DBT oxidation

With 20-fold excess of H_2O_2 over DBT, the oxidation of DBT in the presence **PW–BzPN** was found to be first order in DBT (Figure S9).

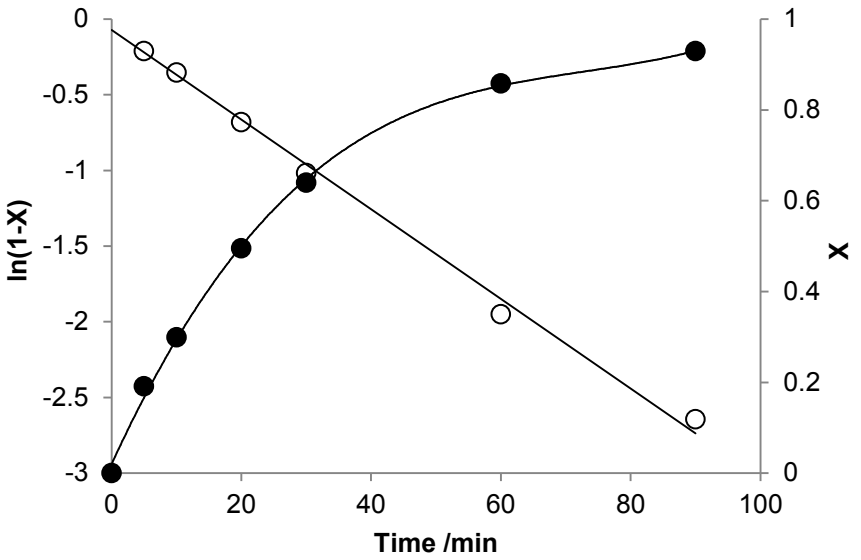

Figure S9 Time course of oxidation of DBT by H_2O_2 in PhMe-H_2O two-phase system the presence of **PW–BzPN**: DBT conversion (X, solid circles) and first-order plot $-\ln(1-X) = kt$ (open circles) (25°C, 0.50 mmol DBT, [DBT]/[POM]=90:1, [H_2O_2]/[DBT]=20:1, [**BzPN**]/[POM]=3.4:1).

Catalyst recovery and reuse

The following procedure was employed for the recovery of **PW–BzPN** catalyst in oxidative desulfurization of DBT. After reaction completion, the reaction mixture was evaporated under vacuum to 1/4 of its volume, and n-hexane was added to refill the original volume. The mixture was left overnight at room temperature to precipitate the catalyst (**PW–BzPN** and **BzPN** are not soluble in hexane). The catalyst was separated from supernatant liquid and washed with hexane using a centrifuge. In the second run, the catalysts showed practically the same performance as in the first run. The DBT sulfone could be quantitatively extracted from the supernatant with polar solvents such as MeCN, DMF, DMSO and 1-methyl-2-pyrrolidone as described elsewhere.[S3, S4] Similar procedure could be used for catalyst recovery in olefin epoxidation.

S3 X. Jiang, H. Li, W. Zhu, L. He, H. Shu, J. Lu, *Fuel* 2009, **88**, 431.
S4 Z. Jiang, H. Lü, Y. Zhang, C. Li, *Chin. J. Catal*. 2011, **32**, 707.